JOURNAL OF PHYSICAL ORGANIC CHEMISTRY, VOL. 8, 387–394 (1995)

KINETIC STUDY OF PROTON/DEUTERON TRANSFER REACTIONS OF 2,4,6-TRINITROTOLUENE AND ITS DERIVATIVES WITH TERTIARY AMINES

YOSHIMI SUEISHI*, TAKANORI FUJIMOTO, TOHRU YOSHIDA, TAKEHARU KURITA, SHUNZO YAMAMOTO AND NORIO NISHIMURA

Department of Chemistry, Faculty of Science, Okayama University, Tshushima, Okayama 700, Japan

The rate of proton/deuteron transfer reactions of 2,4,6-trinitrotoluene (TNT), 2,2′,4,4′,6,6′-hexanitrobibenzyl (HNBB) and 2,4,6-trinitrobenzyl chlorides (TNB) with tertiary amines was followed spectrophotometrically. The rate constants obtained under various conditions were interpreted in terms of isotope, solvent and steric effects. The Arrhenius plots curved upward at low temperatures for TNT and TNB, indicating clearly the intervention of tunnelling. The tunnelling parameters were calculated semi-empirically on the basis of Bell's theory. The observed rate constants at low temperatures agreed well with the predicted values. In the present systems, some side and consecutive reactions involving the formation of 2,2′,4,4′,6,6′-hexanitrostilbene took place, and in some cases interrupted the rate measurements in the proton/deuteron transfer steps.

INTRODUCTION

Reactions involving hydrogen ($H^{\cdot}, H^+, H^-$) transfers are among the most basic types. The kinetic isotope effects for hydrogen transfer reactions are especially interesting, since the involvement of quantum mechanical tunnelling has been invoked to explain the isotopic effect (k^H/k^D) on many occasions. The most extensive work in this field has been carried out on proton/deuteron transfer reactions between general acids and bases. For example, in reactions of 4-nitrophenylnitromethane with tetra- and pentamethylguanidines and 1,8-diazabicyclo[5.4.0]undec-7-ene (DBU), large kinetic isotope effects have been reported.[1–4] In the proton transfer reactions of 2,4,6-trinitrotoluent (TNT) with DBU and other bases, large kinetic isotope effects were also observed.[5–7] For intramolecular hydrogen atom transfer reactions,[8–10] intervention of quantum-mechanical tunnelling has also been put forward. From the pressure effects of the isotropic ratio (k^H/k^D), the quantum-mechanical tunnelling effect for hydride transfer reactions was invoked by Isaacs *et al.*[11,12] for the first time, although a single-step hydride transfer mechanism has been questioned by us.[13]

It has been accepted that the isotope effect $k^H/k^D > 10$ at ambient temperature, the activation energy difference ($E_a^D - E_a^H$) = 4·6–5·7 kJ mol^{-1} and the ratio of the pre-exponential factor $A^D/A^H = 1{\cdot}4$–$2{\cdot}0$ could be regarded as criteria of substantial tunnelling.[1,7,14] Sugimoto and co-workers[5–7] examined pressure, solvent and substituent effects on the proton/deuteron transfer reaction between TNT and bases (Scheme 1). They examined the kinetic isotope effect for the forward reaction at various temperatures and pressures. On the basis of the theory developed by Bell,[14] they calculated the tunnelling correction factor Q, defined as

$$Q = k/k_s \qquad (1)$$

where k is the actual (observed) rate constant and k_s the semi-classical rate constant that would be observed in the absence of tunnelling. They calculated Q and other factors for tunnelling so that these factors reproduce the experimental data well. In this sense, the method could be said to be semi-empirical. Bell's theory predicts that the tunnel effect becomes pronounced as the temperature is lowered and the Arrhenius plot will deviate upwards.

In spite of the prediction of the deviation of the Arrhenius plot, most work has been limited to the linear region of the Arrhenius plot, and very few

---

[*] Author for correspondence.

CCC 0894–3230/95/060387–08

Received 19 September 1994
Revised 16 November 1994

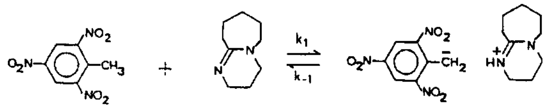

Scheme 1

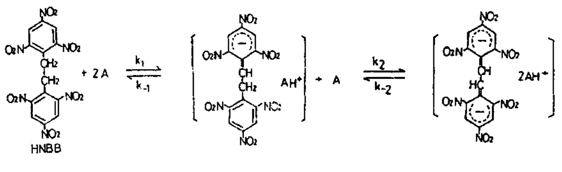

Scheme 2

kinetic studies of the isotope effects in hydrogen[8-10] and proton transfer reactions[1,15] over a wide range of temperatures have been made so far. Indeed, it is difficult to obtain reliable kinetic data at low temperatures and a specially designed cryostat for kinetic measurements is required.

Crampton *et al.*[16] studied extensively the reaction of 2,2′,4,4′,6,6′-hexanitrobibenzyl (HNBB) with various amines. According to them, if tertiary amines are used, hexanitrostilbene (HNS) dianion forms in dimethyl sulphoxide (DMSO) in two steps (Scheme 2).

In spite of the interest in relation to TNT, the isotope effect for HNBB–amine system seems not to have been studied yet. This situation motivated us to study the proton transfer reactions of TNT and its derivatives including HNBB with some tertiary amines, in order to promote better understanding for proton/deuteron transfer reactions.[16] It is of interest to 'see' directly a real deviation of the Arrhenius plot in a low-temperature range, which affords direct evidence for the intervention of tunnelling.

EXPERIMENTAL

Materials. TNT was obtained by nitration of *p*-nitrotoluene in the usual manner and recrystallized three times from ethanol, m.p. 81·5–82·5 °C. TNT-d_3 was prepared according to the literature.[17] By repeating the deuteration process three times, TNT-d_3 with better than 98% isotopic purity in the methyl group was obtained, as determined from its NMR signal. HNBB was prepared by the method of Blatt and Rytina,[18] m.p. 219–221 °C (lit. 218–220 °C); ^{1}H NMR (60 MHz, acetone-d_6), δ 3·64 (4H, s), 9·03 (4H, s). HNBB-d_4 was synthesized from HNBB via three steps by methods similar to the synthesis of TNT-d_3 and recrystallized from acetone, m.p. 219–220 °C; ^{1}H NMR (acetone-d_6), δ 9·03 (4H, s). Hexanitrostilbene (HNS) was prepared by oxidizing HNBB with *p*-benzoquinone in the presence of piperidine in dimethylformamide;[19] ^{1}H NMR (DMSO-d_6), δ 9·07 (4H, s), 7·10 (2H, s) in the ratio of 2 : 1. 1,3,5-Trinitrobenzyl chloride (TNB) was synthesized from TNT[20] and recrystallized from benzene–hexane, m.p. 85·0–85·5 °C; ^{1}H NMR ($CDCl_3$), δ 5·08, 8·88. Reagent-grade 1,8-diazabicyclo[5.4.0]undec-7-ene (DBU), 1,4-diazabicyclo[2.2.2]octane (DABCO), *N,N′*-dimethylpiperadine (DMP) and *N*-methylpiperidine (NMP) were purified by crystallization or distillation under reduced pressure. Reagent-grade dimethyl sulfoxide (DMSO) was dried by allowing it to stand on molecular sieves 4A 1/16 and then distilled under reduced pressure. Dichloromethane (DCM) was dried in the same manner and distilled under atmospheric pressure. Solutions were freshly prepared every day.

Kinetic measurements. All the runs were performed with excess concentrations of amines over acids (more than 25-fold) and the changes in absorbance at λ_{max} in the visible region (530, 500 and 620 nm for deprotonated TNT, TNB and HNBB anions, respectively) were followed spectrophotometrically, and the data were analysed according to pseudo-first-order kinetics, i.e.

$$\ln[(A_e - A)/A_e] = -k_{obsd}t \qquad (2)$$

where A and A_e denote the absorbances of the anions at time t and at equilibrium, respectively. The value of A_e was adjusted by a computer program until the $\ln[(A_e - A)/A_e]$ vs t plot gave a straight line with a correlation coefficient r better than 0·9999.

For the TNB/DBU system, a Union stopped-flow apparatus combined with a Hitachi Model 3200 spectrophotometer was used. For measurements at low temperatures, a specially designed cryostat (Figure 1) was used. The temperature in the reaction cell was controlled within ±0·5 °C.

The reactant solutions were prepared at 25 °C and the concentrations at other temperatures were calibrated using the thermal expansion coefficients of the solvents. The solutions were mixed with the help of a syringe. The observed first-order rate constants k_{obsd} are the means of two to five separate runs, the accuracy being better than 5%. Since the rate was not affected by oxygen as reported,[16] no care was paid to it.

ESR measurements. In order to examine the existence of paramagnetic species which might be formed during the reaction, a JEOL JES-FE3XG spectrometer equipped with a 100 kHz field modulator was used for ESR measurements. Appropriate amounts of HNBB and DABCO in DMSO were mixed in air and placed in the cavity at 25 °C. ESR signals were recorded on the spectrometer.

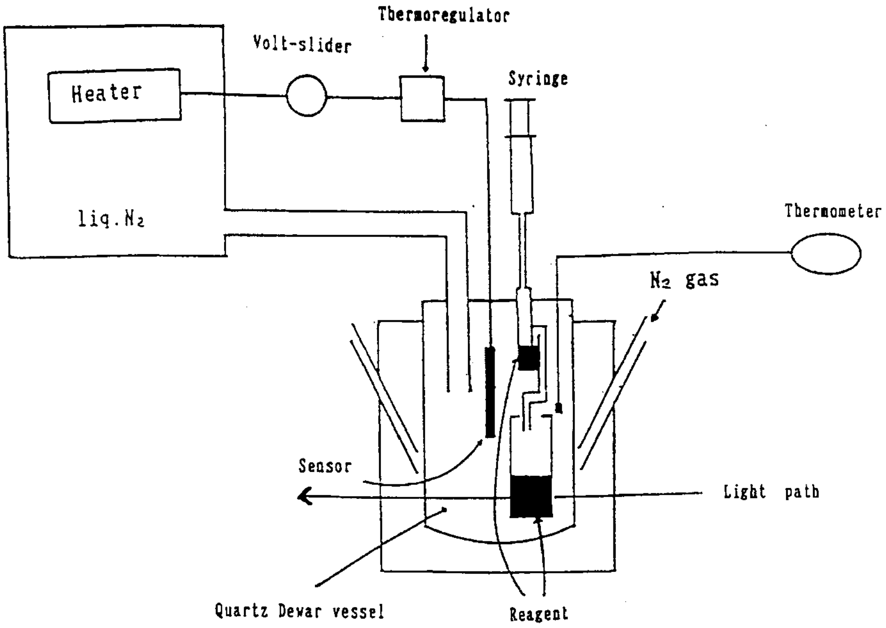

Figure 1. Schematic diagram of spectrophotometric measurement at low temperatures

RESULTS

The plots of the observed first-order rate constant k_{obsd} against the base concentration for TNT and TNB gave straight lines when the base was in large excess. The following general equation has been proposed:[6,7,17]

$$k_{\text{obsd}} = k_1[\text{base}] + k_{-1} \qquad (3)$$

where k_1 and k_{-1} denote the forward and backward rate constants of single proton/deuteron transfer reactions (cf. Scheme 1). Representative plots are shown in Figures 2 and 3. Judging from these figures, the estimation of k_{-1} at each temperature is critical, since values of k_{-1} at lower temperatures are too small to be reliable and are not recorded. Sugimoto *et al.* reported [7,17] that in some cases the estimation of k_{-1} is difficult. From figures in their reports, the enthalpy of reaction ΔH was estimated to be ca. -20 kJ mol^{-1} for TNT/1-phenylpiperidine in acetonitrile, and -56 kJ mol^{-1} for TNT/DBU in 1,2-dichloroethane (DCE). The value $\Delta H = 31$ kJ mol^{-1} for TNT/DBU in DCM was obtained when we tentatively used only the data at -10 and -20°C. It could be said therefore that proton-transfer reactions to form ion pairs are certainly exothermic as expected by enhanced solvation.

For the HNBB–DABCO system, the absorption band at *ca* 630 nm assigned to the corresponding HNS dianion[16] appeared in DMSO and other polar solvents (Scheme 2). The formation of the dianion is inferred according to Scheme 2. In this scheme, the rate-determin-

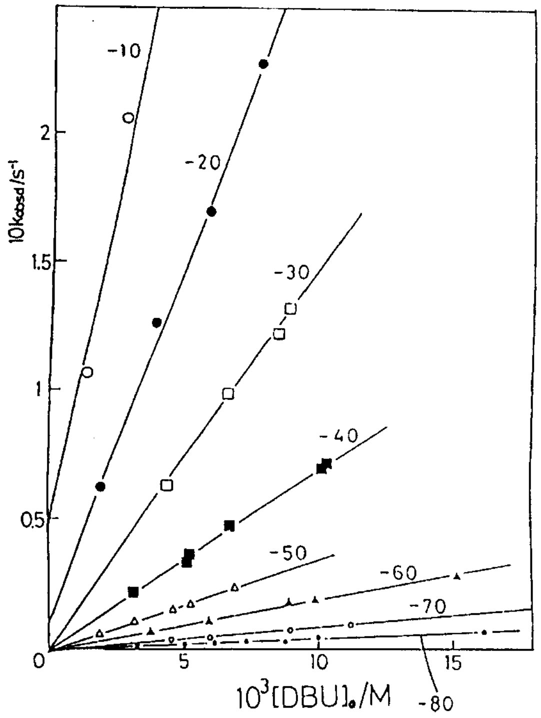

Figure 2. Plots of k_{obsd} against $[\text{DBU}]_0$ for the reaction of TNT with DBU at various temperatures in DCM; 10^5 $[\text{TNT}]_0 = 3{\cdot}38\text{–}10{\cdot}3$ mol dm^{-3}

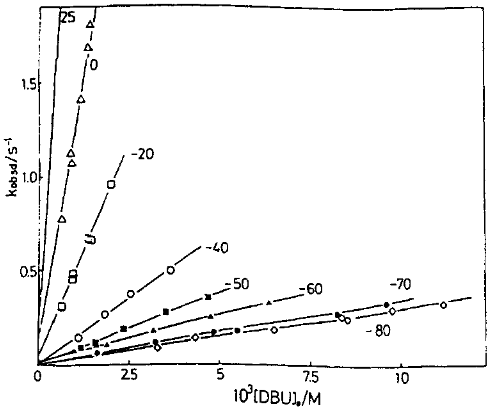

Figure 3. Plots of k_{obsd} against $[DBU]_0$ for the reaction of TNB with DBU at various temperatures in DCM; $10^5[TNB]_0 = 1{\cdot}40–7{\cdot}12$ mol dm^{-3}.

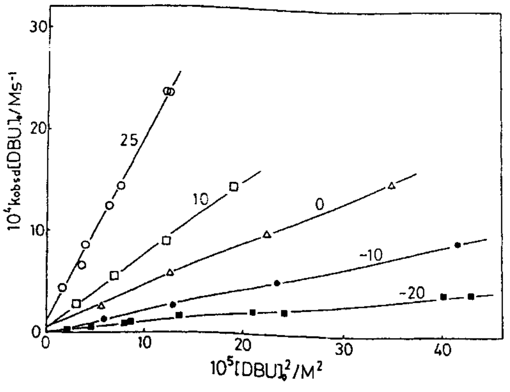

Figure 4. Plots of $k_{obsd}[DBU]_0$ against $[DBU]_0^2$ for the reaction of HNBB with DBU at various temperatures according to equation (5); $10^5[HNBB]_0 = 2{\cdot}44–8{\cdot}36$ mol dm^3.

Table 2. Rate constants $10^2 k_1$/dm^3 mol^{-1} s^{-1} for the reactions of HNBB and HNBB-d_4 with cyclic tertiary amines in DMSO

Temperature/°C		DMP	MP	DABCO	DBU[a]
25	H	1·51	2·94	114[b]	1820
	D	0·117		14·3	121
35	H	2·38	4·58	140	
	D	0·214		17·8	
45	H	4·14	6·67		

[a] In DCM (see Table 1).
[b] Reported value is 110.[16]

ing step is involved in the first proton transfer step, followed by the very fast second proton transfer.[16] Therefore, a steady-state assumption can be made for the monoanion. The apparent pseudo first-order rate constant k_{obsd} for the formation of the ion pair can be given by

$$k_{obsd} = k_1[\text{base}]_0 + k_{-1}k_{-2}/k_2[\text{base}]_0 \qquad (4)$$

For the sake of a convenient plot, this equation can be rearranged as follows:

$$k_{obsd}[\text{base}]_0 = k_1[\text{base}]_0^2 + k_{-1}k_{-2}/k_2 \qquad (5)$$

According to this equation, the plots of $k_{obsd}[\text{base}]_0$ against $[\text{base}]_0^2$ should give a straight line at each temperature, which was confirmed by the experimental results. Some examples are shown in Figure 4.

From the slopes, the rate constants for the first forward step were estimated. In Table 1, the k_1 values in DCM at various temperatures are given, and in Table 2 the k_1 values for the HNBB–amine system in DMSO are given.

Sugimoto and coworkers[17] have already studied the proton transfer reaction for the TNT/DBU system in the temperature range 5–30°C. They reported that

Table 1. Second-order rate constants (k_1/dm^3 mol^{-1} s^{-1}) for the reactions of TNT, HNBB and TNB with DBU in DCM

Temperature/°C	TNT	TNT-d_3	HNBB	HNBB-d_4	TNB
25			18·2	1·21	2980
20				0·772	
10			7·29	0·413	
5				0·283	
0			4·26		1120
−10	52·0	1·91	2·21		
−20	27·9	0·888	0·955		452
−30	14·8	0·372			
−40	6·85	0·137			135
−50	3·42				73·0
−60	1·89				47·5
−70	0·874				32·6
−80	0·426				28·9

k_1(dm^3 mol^{-1} s^{-1}) at 25°c was 204 in acetonitrile, 565 in DCE, and 41·8 in DCM. Although we have carried out our kinetic study over a much lower temperature range, their data in DCM are considerably smaller than those expected from our Arrhenius plot. Possible reasons for it may arise from different source of the solvent DCM and its degree of purity. It is known that cholorocomponds are photosensitive leading to contamination. Indeed, it would be very difficult to explain their kinetic data simply in terms of solvent polarity. Freshly distilled solvents DCM and DMSO were used in every run, otherwise the kinetic reproducibility was poor.

DISCUSSION

Kwart[21] pointed out that it is dangerous to deduce a mechanistic conclusion from a single temperature measurement of k^H/k^D, and that whether an isotope effect is large, small, or intermediate is devoid of significance until its temperature dependence is also known. However, simultaneous measurements of k^H and k^D over a wide range of temperatures are very difficult. Although, because of experimental limitations, the rate data for H and D are not complete over the full temperature ranges in Tables 1 and 2, we wish to discuss the significance of the primary isotope effect from the temperature dependence of k_1^H and k_1^D.

Calculation of tunnelling parameters

The Arrhenius expression for the actual rate constant k is given by

$$k = Qk_s = WA_s \exp(-E/RT) \tag{6}$$

where E is the height of the barrier and A_s is the pre-exponential factor that would be found in the absence of tunnelling. The expression derived by Bell[14] for a symmetric parabolic barrier is

$$Q = \frac{0{\cdot}5u}{\sin(0{\cdot}5u)} - \sum_{n=1}^{\infty} (-1)^n \frac{\exp[(u-2n\pi)a/u]}{(u-2n\pi)/u} \tag{7}$$

where $a = E/RT$, $u = h\nu/k_BT$ and $\nu = (E/2M)^{1/2}/\pi b$; b is the half-width of the barrier at the base and ν is the frequency of oscillation of a particle of mass M reduced to 1 mol in a parabolic potential. On the reasonable assumption that A_s is the same for H and D, the ratio k^H/k^D can be calculated by using the equation

$$(k^H/k^D)_{\text{calcd}} = (Q^H/Q^D)\exp[(E^D - E^H)/RT] \tag{8}$$

The calculation was made in the following manner. (1) It was assumed that a bare H or D moves, so that $M^H = 1$ g mol^{-1} and $M^D = 2$ g mol^{-1}. (2) We chose a set of values for E^H, E^D and b^H with the restriction of $(E^D - E^H) \leq 5{\cdot}7$ kJ mol^{-1}; b^D is automatically determined by the relationship $b^D = b^H(E^D/E^H)^{1/2}$, since the force constant should be the same for H and D. It is not reasonable to assume that b is the same for H and D,[1,5–7] since the assumption leads to a change in the force constant and hence curvature at the top of the barrier. (3) The higher order terms of $n > 4$ in equation (7) were neglected. (4) A set of these values was varied with the help of a computer until we obtained values of $(k^H/k^D)_{\text{calcd}}$ that best reproduced the experimental $(k^H/k^D)_{\text{obsd}}$ values.

In the liquid phase, the particle being transferred might be coupled with solvent molecules, which gives rise to an increase in the effective mass and, therefore, the probability of tunnelling will be decreased. However, according to recent work,[22] solvent polarity does not exert serious effects on tunnelling. Therefore, the above assumption of the effective mass for H and D would not lead a serious mistake, as evidenced by the results mentioned below.

Tunnelling phenomena at low temperatures

In the case of the TNT(H and D)–DBU system, the rate data over the temperature range −10 to −40 °C were used for the calculation of tunnelling parameters, and these were used for the prediction of the rate constants at lower temperatures.

The calculated rate constants and the tunnelling correction factors are given in Table 3, together with the Arrhenius parameters. It is noted that the values for k_1 and Q at lower temperatures were calculated using the data above −40 °C. The k^H/k^D value at 25 °C predicted from the Arrhenius parameters is 15·7, which considerably exceeds the semi-classical limit. Figure 5 shows the Arrhenius plot for H and D transfers. The dashed lines are those calculated semi-empirically using the procedures stated above. We see that the experimental points for H transfer in the lower temperature region fall on the predicted line. Although the Q values for D are indicative of the involvement of tunnelling, the Arrhenius plot is apparently almost linear over the temperature range −10 to −80 °C for D transfer. The above findings unambiguously show that there is a

Table 3. Arrhenius parameters for TNT, HNBB and TNB calculated by using the data in Table 1

Parameter	TNT	HNBB	TNB
E_a^H/kJ mol^{-1}	34·3 ± 0·4	0·4 ± 0·7	27·5 ± 0·3
E_a^D/kJ mol^{-1}	44·8 ± 0·5	48·6 ± 1·7	
LnA^H	19·7 ± 0·2	19·2 ± 0·3	19·1 ± 0·1
LnA^D	21·1 ± 0·3	19·7 ± 0·7	
$E_a^D - E_a^H$	10·5	8·2	
A_D/A_H	4·1	1·7	
k_1^H/k_1^D	39·7 (243 K)	15·8 (298 K)	

significant contribution of tunnelling in this system. The Arrhenius plots for the reactions of HNBB, HNBB-d_4 and TNB with DBU are shown in Figure 6. The plots were limited within a comparatively narrow range of temperatures for the HNBB–DBU system, since a side reaction was substantiated at lower temperatures, as exemplified by the appearance of absorptions in the vicinity of 460 and 520 nm, and this made the exact estimation of the rate of formation of the dianion impossible. Similar bands were also observed for the HNBB-d_4–MP in DMSO system; this will be discussed later. Although each Arrhenius plot is apparently linear over this temperature range, the calculated tunnelling parameters in Table 3 clearly show the intervention of tunnelling in this system also.

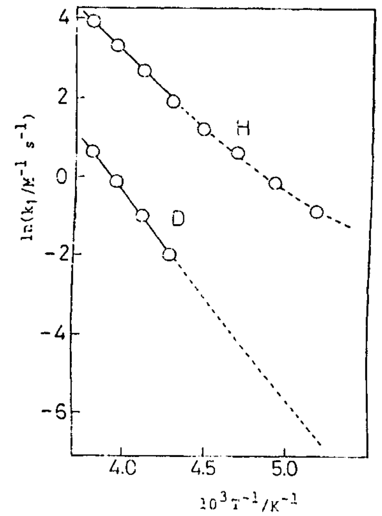

Figure 5. Arrhenius plots for the reactions of TNT and TNT-d_3 with DBU in DCM. Dashed lines are those predicted from the theory of the tunnel effect

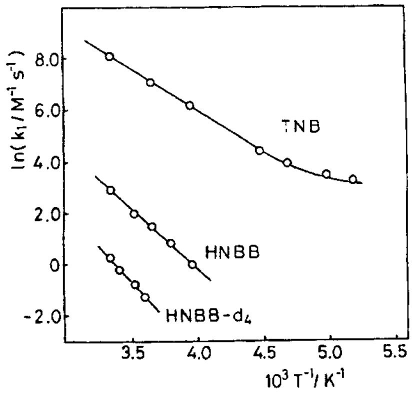

Figure 6. Arrhenius plots for the reactions of HNBB, HNBB-d_4 and TNB with DBU in DCM

Unfortunately, we were unsuccessful in synthesizing TNB-d_3. However, the Arrhenius plot for TNB (Figure 6) clearly shows substantial tunnelling at low temperatures. It could be concluded that the tunnelling is embodied unambiguously in all the above systems.

Effects of steric hindrance, solvent polarity and basicity of amines on the rate of reaction

If we inspect the data in Tables 1–3, the following points can be noted. The rate for HNBB is considerably smaller than that for TNT. A severer steric hindrance of HNBB compared with TNT would prevent the approach of the nitrogen base centre and increase the barrier height and width (Table 4). Indeed, the experimental value of the activation energy for HNBB is greater than that for TNT.

Similar steric arguments could be made for the structure of amines in the HNBB-amine system. In the cases of DMP and MP, the rates are much smaller than those for DABCO and DBU. The nitrogen atoms in DABCO and DBU are fixed within molecules and inner rotations around the nitrogens are forbidden. Meanwhile, methyl group(s) can rotate around the nitrogens in MP and DMP, and this would disfavour the access of HNBB molecules. In spite of the lower basicity of DABCO ($pK_a = 8{\cdot}8$ in H_2O) compared with that of MP ($pK_a = 11{\cdot}2$ in H_2O), the rate is much greater for the former than the latter. Therefore, the steric effects must overwhelm the effects of basicity. In this respect, it is worth noting that 1,8-dimethylaminonaphthalene ('proton sponge,' $pK_a = 12{\cdot}3$ in H_2O) did not react with HNBB at all, in spite of its high basicity, since the amino nitrogens are presumed to be highly blocked.

In Table 2, we see that the rate for the HNBB–DBU system in DCM is much greater than that in DMSO. From the viewpoint of a general solvation concept, the opposite results may be expected, since charge separation occurs on going from the ground to the transition state, and this will give rise to a greater free energy depression due to solvation in DMSO than in DCM. In fact, this is not the case. According to our view, a special solvation effect[23,24] such as hydrogen bonding between the acidic methylene hydrogens and the oxygen

Table 4. Tunnelling parameters

Parameter	TNT	HNBB
E^H/kJ mol^{-1}	41·7	45·8
E^D/kJ mol^{-1}	47·4	51·5
b^H/nm	5·72	6·04
b^D/nm	6·10	6·40
ν^H/cm^{-1}	847	843
ν^D/cm^{-1}	599	595
Q^H (−20 °C)	3·60	3·50
Q^D (−20 °C)	1·72	1·70

on DMSO is operating, and this prohibits the access of DBU to the reaction centre.

The rate for TNB is much greater than that for TNT at each temperature. This could certainly be attributed to the more electronegative nature of the chlorine atom, which gives rise to enhanced deprotonation. It is noted that a statistical correction for the number of hydrogens being abstracted should be made for exact arguments, although this was not done in this work.

Success and side reactions for the HNBB–amine systems

When the amines are present in great excess over HNBB, the maximum concentration of DA^{2-} during the reaction could be approximated as the initial concentration of HNBB, since the colour fading is not so rapid. From this approximation, the molar absorptivity of DA^{2-} was presumed to be $44\,000 \pm 300\ dm^3\ mol^{-1}\ cm^{-1}$, which agreed well with the reported value ($42\,000\ dm^3\ mol^{-1}\ cm^{-1}$).[25]

Strickly speaking, the HNBB–Amine system involves side and successive reactions. When the reaction temperature is lowered below -20°C for the HNBB–DBU system, new peaks appeared at ca. 460 and 520 nm besides the peak due to the dianion in the initial stage of reaction and in this case the first-order plot was unsuccessful. In the case of the HNBB-d_4/MP system in DMSO, these new peaks appeared from the beginnig and this made the estimation of the concentration of dianion impossible. In other cases, where peaks appeared their intensities were negligibly small in the early stage of reaction, and did not disturb the first-order kinetic treatment.

Figure 7 shows that the coloured dianion fades slowly after its absorbance at 650 nm has reached a maximum, and simultaneously a new absorption band appears at 525 nm (sh), 493 nm and 390 nm with a different rate. The final spectrum agreed roughly with that of an HNS–DABCO reaction mixture, as shown in Figure 8. Russel and Janzen[26] suggested that the dianions reacts with dissolved oxygen to yield HNS and O_2^{2-}:

$$DA^{2-} + O_2 \rightarrow HNS + O_2^{2-}$$

In the Experimental section, it was shown that HNS was prepared by the base-catalysed oxidation of HNBB by *p*-benzoquinone. Taking these situations into account, it is very plausible that the HNS is formed from the dianion and it reacts further with DABCO to form a final product(s):

$$HNS + DABCO \rightarrow \text{final product(s)}$$

The overall reaction scheme is complicated by the appearance of ESR signals during the reaction and an unidentified spectrum appeared at low temperatures in some cases. It has been reported that for the HNBB–amine systems no ESR signal was detected.[16] However, we observed ESR signals for the present systems, and examples are shown in Figure 9. Figure 9(a) shows that the signal consists of two components, one a triplet of doublets and the other poorly resolved. The former signal clearly indicates that one nitrogen and one hydrogen ($a_N = 0{\cdot}45$ and $a_H = 0{\cdot}16$ mT) are contributing to the signal. Figure 9(b) is attributable to other species and Figure 9(c) could be regarded as the same kind of species as that in Figure 9(a). The disappearance of the doublet could be ascribed to the reduced hyperfine coupling constant for D, as expected from the Fermi theory ($a_H/a_D = 6{\cdot}5$). However, the assignments of these signals are very difficult, since the a_N value is extremely small and there have been no comparable data for presuming the observed radical structure. What can be said is that these signals are surely responsible for species which came from HNBB and not from the amines used.

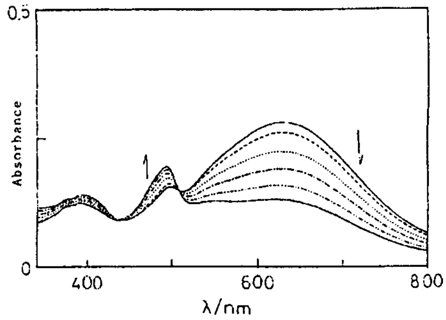

Figure 7. Time dependence of the absorption spectra for the reaction of HNBB with DABCO in DMSO at 25 °C. $[HNBB]_0 = 9{\cdot}91 \times 10^{-6}\ mol\ dm^{-3}$; $[DABCO]_0 = 2{\cdot}28 \times 10^{-2}\ mol\ dm^{-3}$. Time from top to bottom: 4·5, 5·5, 7·5, 9·5, 11·5, 13·5 h

According to the report of Crampton and coworkers,[16] primary and secondary amines react with HNBB to form σ-adducts (λ_{max} 450, and 515 nm) followed by conversion into the HNBB dianion. Although they reported

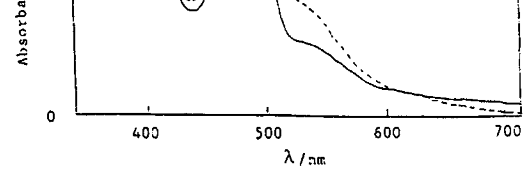

Figure 8. Final spectra of HNBB–DABCO (dashed line) and HNS–DABCO (solid line) mixtures in DMSO

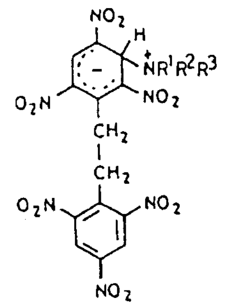

that tertiary amines react with HNBB to form the HBNN dianion directly without forming σ-adducts, we tentatively assign the bands observed in the vicinity of 460 and 520 nm at low temperatures to the zwitterionic species such as that shown.

In this connection, the work of Buncel and Menon[27] is worth noting. They studied the reactions of *p*-nitrotoluene with bases and showed that a sequence of consecutive events involving proton and electron transfer processes takes place. In the light of their results, together with the above findings, the present reaction is exceedingly complicated by the intervention of some side and consecutive reactions and in some cases this made the exact determination of the rate constants in the proton transfer step impossible.

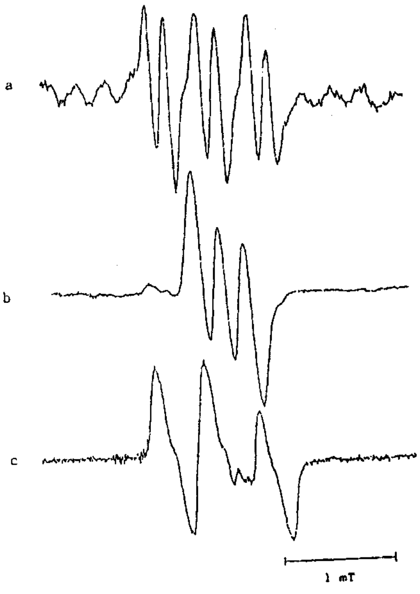

Figure 9. (a) ESR signals appeared in the initial stage of reaction for the HNBB–DABCO system. (b) ESR signal appearing after the first signal had disappeared. (c) ESR signal appearing in the initial stage of reaction for the HNBB-d_4–DABCO system

In spite of such situations it may be concluded that quantum mechanical tunnelling is surely involved in the main reactions in the initial proton/deuteron transfer steps in our systems.

REFERENCES

1. E. F. Caldin and S. Mateo, *J. Chem. Soc., Faraday Trans. 1* **71**, 1876 (1975).
2. E. F. Caldin and O. Rogne, *J. Chem. Soc., Faraday Trans. 1* **74**, 2065 (1978).
3. O. Logne, *Acta Chem. Scand., Ser. A* **32**, 559 (1978).
4. J. H. Blanch, O. Rogne and L. I. Rossemyr, *J. Chem. Soc., Faraday Trans. 1* **76**, 1905 (1980).
5. N. Sugimoto, M. Sasaki and J. Osugi, *J. Am. Chem. Soc.* **105**, 7676 (1983).
6. N. Sugimoto, M. Sasaki and J. Osugi, *J. Chem. Soc., Perkin Trans. 2* 655 (1984).
7. N. Sugimoto and M. Sasaki, *J. Chem. Soc., Faraday Trans. 1* **81**, 1441 (1985).
8. G. Brunton, D. Griller, L. R. C. Barclay and K. U. Ingold, *J. Am. Chem. Soc.* **98**, 6803 (1976).
9. G. Brunton, L. R. C. Barclay, D. Griller and K. U. Ingold, *J. Am. Chem. Soc.* **100**, 4197 (1978).
10. V. Malatesta and K. U. Ingold, *J. Am. Chem. Soc.* **103**, 3094 (1981).
11. N. S. Isaacs, K. Javaid and E. Lannala, *Nature (London)* **268**, 372 (1977).
12. N. S. Isaacs, K. Javaid and E. Lannala, *J. Chem. Soc., Perkin Trans. 2* 709 (1987).
13. Y. Osawa, N. Nishimura and S. Yamamoto, *Bull. Chem. Soc. Jpn.* **64**, 2648 (1991), and references cited therein.
14. R. P. Bell, *The Tunnel Effect in Chemistry*. Chapman and Hall, London (1980).
15. J. Hennig and H. Limbach, *J. Chem. Soc., Faraday Trans. 2* **75**, ••• (1979).
16. M. R. Crampton, P. J. Routledge and P. Golding, *J. Chem. Soc., Perkin Trans. 2* 1421 (1984), and references cited therein.
17. N. Sugimoto, M. Sasaki and J. Osugi, *J. Phys. Chem.* **86**, 3418 (1982).
18. A. H. Blatt and A. V. Rytina, *J. Am. Chem. Soc.* **72**, 403 (1950).
19. G. P. Sollott, M. Warman and E. E. Gilbert, *J. Org. Chem.* **44**, 3328 (1979).
20. K. G. Shipp and L. A. Kaplan, *J. Org. Chem.* **31**, 857 (1966).
21. H Kwart, *Acc. Chem. Res* **15**, 401 (1982).
22. P. Priszynski and A. Jarczewski, *J. Chem. Soc., Perkin Trans. 2* 1117 (1986).
23. N. Nishimura, T. Moriya, Y. Okana, K. Tanabe, K. Kawabata and T. Watanabe, *Bull. Chem. Soc. Jpn.* **50**, 1969 (1977).
24. N. Nishimura, K. Okahashi, T. Yukutomi, A. Fujiwara and S. Kubo, *Aust. J. Chem.* **31**, 1201 (1978).
25. M. R. Crampton and P. J. Routledge, *J. Chem. Res. (S)* 314 (1983).
26. G. A. Russel and E. G. Janzen, *J. Am. Chem. Soc.* **89**, 300 (1967).
27. E. Buncel and B. C. Menon, *J. Am. Chem. Soc.* **102**, 3499 (1980).